Published in final edited form as:
Nat Methods. 2013 February ; 10(2): 125–127. doi:10.1038/nmeth.2301.

Conditional genome engineering in *Toxoplasma gondii* uncovers alternative invasion mechanisms

Nicole Andenmatten[1,*], **Saskia Egarter**[1,*], **Allison J Jackson**[1,*], **Nicolas Jullien**[2], **Jean-Paul Herman**[2], and **Markus Meissner**[1,#]

[1]Division of Infection and Immunity, Institute of Biomedical Life Sciences, Wellcome Centre for Molecular Parasitology, Glasgow Biomedical Research Centre, University of Glasgow, 120 University Place, Glasgow G12 8TA, UK.

[2]ICNE-UMR 6544 Centre National de Recherche Scientifique (CNRS), Université de Méditerranée, Marseille, France.

Abstract

We established a conditional site–specific recombination system based on dimerizable Cre–mediated recombination in the apicomplexan parasite *Toxoplasma gondii.* Using a novel single vector strategy that allows ligand-dependent, efficient removal of a gene of interest, we generated three knockouts of apicomplexan genes considered essential for host-cell invasion. Our findings uncover the existence of an alternative invasion pathway in apicomplexan parasites.

Several strategies have been established to generate conditional mutants for genes in the apicomplexan parasite *Toxoplasma gondii* [1,2]. However, background expression levels can obscure mild phenotypes. Due to this inherent problem, the essential nature of a gene of interest (GOI) cannot be answered with certainty. The current model of gliding motility and active host cell invasion, for example, has been well supported by the generation of knockdown mutants for crucial components of the parasite's actin-myosin system using a tetracycline–inducible transactivation system[3]. Intriguingly, these mutants show only a reduction, not an absence, of host-cell invasion [3-8], leading us to question if these genes are indeed essential.

To generate knockouts (KOs) of diverse invasion factors, we established the DiCre system [9] in *T. gondii*. This system is based on site–specific recombination using dimerizable Cre recombinase. Cre recognises and catalyses the excision of DNA flanked by two identical 34 bp sequences known as loxP sites. Here, Cre is split into two inactive fragments that are fused to rapamycin binding proteins FRB and FKBP, respectively. Addition of the ligand rapamycin, results in reconstitution of the functional enzyme, and excision of the floxed GOI (Fig. 1a). We co-expressed both Cre subunits in wild type RH *hxgprt*$^-$ parasites (RH DiCre, Fig. 1b) and tested rapamycin–dependent excision of floxed *lacZ* in this recipient strain (RH BloxP, Fig. 1c). Without rapamycin, we did not identify any *lacZ* excision, however, when the parasites were incubated with 50 nM rapamycin, after 24 hours we detected a 90 % excision rate using X-Gal staining (Fig. 1c). Importantly, *lacZ* deletion

[#]Correspondence should be sent to markus.meissner@glasgow.ac.uk Tel.: +44 141 330 6201 .
[*]These authors contributed equally to this work

Author contributions N.A. established the DiCre system, generated and analysed the *myoA* KO parasites. A.J.J. generated and analysed the *mic2* KO. S.E. generated and analysed the conditional *act1* KO. N.J. and J.P.H. shared confidential information for the establishment of the DiCre system. M.M. initiated and guided this study. M.M., A.J.J., N.A. and S.E. wrote the manuscript.

The authors declare they have no competing financial interests.

Europe PMC Funders Author Manuscripts

cannot be observed upon induction with high doses of the rapamycin analogue Shield–1, the inducer of the ddFKBP–system [1] (Fig. 1c). We found that one-hour incubation with rapamycin is sufficient for efficient *lacZ* excision (Fig. 1d). Next we designed a gene-swap strategy, where loxP sites flank the cDNA of a GOI. Removal of the cDNA by Cre–mediated recombination positions the YFP under control of the constitutive promoter, resulting in green fluorescent parasites (Fig. 1e). We tested this strategy by transfecting RH DiCre parasites with a vector containing floxed *KillerRed* 10. Parasites incubated in the presence of rapamycin displayed a highly efficient switch from red- to green-fluorescent parasites (96 %), as demonstrated by microscopy and FACS analysis (Fig. 1f,g). We have successfully employed this strategy to generate an arsenal of KO mutants. Importantly, this strategy allows visual identification of YFP positive KO parasites after successful GOI removal. Furthermore, we generated a parental strain, *ku80::diCre*, where homologous recombination is favoured (Supplementary Fig. 1).

Next we applied this technology to functionally dissect critical components of the parasites' invasion machinery. We generated conditional KO mutants for the gliding motor, myosin A (MyoA), the micronemal protein MIC2, and parasite actin (Act1; Fig. 2a and Supplementary Figs. 2–5). These invasion factors are considered essential for host-cell invasion based on the interpretation of phenotypes obtained in knockdown (MyoA [3] and MIC2 [8]) or overexpression mutants (Act1 [11]). To produce the conditional *myoA* KO parasites, firstly we introduced a second floxed and ty–tagged copy of *myoA* (regulated by the chimeric promoter p5RT70) [12], randomly into the genome of the RH DiCre parasites. The endogenous *myoA* was then replaced with the *cat* gene, producing parasites containing only one copy of *myoA* (Supplementary Fig. 2). For *mic2* and *act1* we directly employed the gene-swap strategy in *ku80::diCre* and exchanged the endogenous GOI for the gene-swap construct, where expression of the respective cDNA is under the endogenous promoter's control (Supplementary Figs. 4 and 5). We verified all genomic modifications using analytical PCR on genomic DNA (Supplementary Figs. 2–5). The parasite strains containing floxed versions of the GOI (loxPMyoA, loxPMic2 and loxPAct1) did not show any detectable phenotype. (Fig. 2a,b and Supplementary Figs. 2–5). In contrast, Cre–activation with 50 nM rapamycin for 4 – 8 hours resulted in a mixed population consisting of uninduced and knockout parasites for all three lines (Fig. 2a and Supplementary Figs. 2–5). The excision efficiency was dependent on the strain; loxPMyoA displayed the most efficient recombination of ~ 75 %, loxPMic2 approximately 40 % and the recombination rate in the loxPAct1parasites was about 20 %, when analysed 24 – 36 hours after induction. Given that KO parasites are expressing YFP, it is straightforward to perform phenotypic characterisations of the respective conditional KO, or to enrich this population using FACS sorting (Supplementary Fig. 5 and data not shown).

Surprisingly, although we verified that the conditional *myoA* KO has similar egress, gliding motility, and host cell invasion phenotypes as previously described for a *myoA* knockdown mutant (Supplementary Fig. 2) [3], we successfully isolated a clonal *myoA* KO parasite line that can be permanently maintained in culture. Similarly, we achieved isolation of a clonal *mic2* KO parasite line, demonstrating for the first time that neither *myoA* nor *mic2* are essential for parasite survival. This suggests the existence of a MIC2– and MyoA–independent invasion mechanism (Fig. 2a,b). We verified the absence of the respective genes using analytical PCR on genomic DNA and absence of the proteins in Western blots and IFA for both clonal KO lines (Fig. 2a and Supplementary Figs. 3 and 4). In a growth assay of *myoA* KO and *mic2* KO parasites we could see that both KO strains displayed a significant growth defect that was more pronounced for *myoA* KO parasites when compared to control parasites (Fig. 2a,b). Importantly, the reintroduction of *myoA* led to full complementation of *myoA* KO parasites, demonstrating a specific phenotype (Supplementary Fig. 3). Interestingly, MyoA deletion did not affect secretory organelles or

localisation of other glideosome components, such as the myosin light chain 1 (MLC1) or the Gliding Associated Protein 45 (GAP45; Fig. 2c). Immunofluorescence analysis of *mic2* KO parasites showed the absence of MIC2 (Fig. 2a), while other micronemal proteins AMA1 and MIC3 remained unaffected and displayed normal localisations (Fig. 2d and Supplementary Fig. 4). As described previously for a MIC2 knockdown, the localisation of MIC2's interaction partner, M2AP, and its unprocessed form was severely disrupted [8], and could be found in punctate spots within the parasite in addition to the parasitophorous vacuole (Fig. 2d and Supplementary Fig. 4).

In contrast to MyoA and MIC2, we were unable to isolate a clonal *act1* KO parasite line, demonstrating that actin is essential for parasite survival. We never observed any plaques formed by YFP positive *act1* KO parasites upon induction of loxPAct1 (Fig. 2a and Supplementary Fig. 5). An immunofluorescence time-course of YFP parasites in the induced loxPAct1 population established that Act1 protein levels are significantly decreased as early as 24 hours after induction and are undetectable after 72 hours (Fig. 2e). Although a role of Act1 in parasite replication has been questioned previously [13], we found that Act1 depletion resulted in a strong apicoplast segregation defect – a plastid-like organelle (Fig. 2e). No other gross morphological consequences were obvious (Fig. 2e and Supplementary Fig. 5). Intriguingly, we found that green–fluorescent parasites can be easily identified in the induced loxPAct1 population up to 10 days after induction, indicating host-cell invasion in the absence of Act1. Indeed, when parasites are released from the host cell 72 hours after induction, the *act1* KO parasites remain capable of infecting host cells (Fig. 2e). However, these parasites died within the host cell due to apicoplast loss, resulting in a typical delayed death phenotype [14].

In summary, the DiCre system enables the efficient generation of conditional KO mutants with a clear and interpretable phenotype, as background expression of the GOI can be excluded. We present here three KO examples of genes previously described as essential for host-cell invasion and demonstrate that the parasite is capable of employing alternative invasion mechanism(s). MyoA and MIC2 are shown to be dispensable for host-cell invasion. A few remaining actin molecules could enable invasion, but since a striking effect on apicoplast replication can be observed as early as 24 hours after *act1* excision, we consider this possibility unlikely. Instead, we favour the interpretation that *T. gondii* is capable of employing an Actin/MyoA/MIC2-independent mechanism to invade the host cell. Future studies will elucidate this novel finding in detail.

This conditional knockout technology provides researchers with a novel tool that produces complete KO for the analysis of essential genes. Our understanding of *T. gondii* invasion has been remodelled as a result of this technology. Consequently our study necessitates re–analysis of previously described "essential" invasion factors, to define the minimal invasion machinery. We have successfully adapted the DiCre system for the malarial parasite *Plasmodium falciparum* (Collins *et al.*, unpub. data), demonstrating the potential of this technology to enhance all apicomplexan biological research.

Methods

Cloning of DNA constructs

All primers used in this study are listed in Supplementary Table 1. The *FKBP–Cre59* open reading frame (ORF) consists of *NLS*, *FKBP12*, linker and *Cre1–59*; *FRB–Cre60* ORF consists of *NLS*, *FRB T2098L*, linker and *Cre60–343* [9]. The respective ORFs were amplified using the primers FRB–Cre60/ FKBP–Cre59 fw and FRB–Cre60 rv or FRB–Cre60/ FKBP– 59 fw and FKBP–Cre59 rv and cloned into the plasmid *p5RT70mycGFPPfMyoAtailTy–HX* [15] using EcoRI and PacI as restriction sites

(*p5RT70FKBPCre59–HX*; *p5RT70FKBPCre60– HX*). In case of *p5RT70FKBPCre59–HX*, *hxgprt* was exchanged for *dhfr* derived from *pDHFR–Tsc3* 16 via SacII (*p5RT70FKBPCre59–DHFR*). To generate a plasmid for integration of both Cre subunits into the same genomic locus, *FKBP–Cre59* was amplified with the primers p5RT70FKBPCre59 fw and rv using *p5RT70FKBPCre59–DHFR* as template. The resulting p5RT70FKBPCre59 fragment was cloned into *p5RT70FFRBCre60– HX* using KpnI (*p5RT70DiCre–HX*). Finally the *hxgprt* resistance gene was exchanged for *dhfr* via SacII. The resulting vector is referred to as *p5RT70DiCre–DHFR*.

To generate *ploxPTyMyoAloxP–DHFR*, the expression cassette *p5RT70TyMyoA*, which allows expression of N–terminal Ty–tagged MyoA, has been placed between the two LoxP sites of *pLox–P30/11LacZ–Lox–CAT* [17] using ClaI and PacI. The *CAT* selection cassette on this vector was exchanged for *dhfr* from *pDHFR–Tsc3* using NotI and XbaI as restriction enzymes resulting in the construct *p5RT70loxPTyMyoAloxP–DHFR*.

A *ku805′UTR–DiCre–ku80 3′UTR* cassette was constructed in order to replace the *hx* ORF by *diCre* in *ku80::hx* strain [18]. For this purpose, the 5′UTR and the 3′UTR of *ku80* locus were amplified using ku80 5′UTR fw/rv or ku80 3′UTR fw/rv primer pairs, respectively. Afterwards the amplified fragments were cloned into *p5RT70ddmycGFPPfMyoAtailTy–HX* [15] using Kpn1/SpeI and SpeI/SacII restriction sites. Finally, the DiCre expression construct from *p5RT70DiCre–DHFR* was placed between the 5′UTR and 3′UTR of *ku80* using SpeI. The gene-swap vector *p5RT70loxPKillerRedloxPYFP–HX* was generated by cloning *KillerRed* [10] into *p5RT70mycGFPPfMyoAtailTy–HX* [15]. To introduce a loxP site upstream of *KillerRed*, the promoter region was amplified using p5RT70 fw and rv primers. The amplified promoter fragment was placed upstream of *KillerRed* using KpnI and ApaI. To introduce a loxP site and YFP downstream of the *KillerRed* STOP codon, *YFP* was amplified from *p5RT70ddYFP–CAT* 1 using LoxPYFP fw and rv primers. The fragment was then placed downstream of *KillerRed* using PacI and NotI.

To generate *loxPMic2loxP–YFP–HX*, the parental vector *p5RT70loxPKillerRedloxPYFP–HX* was modified such that the *mic2* 3′UTR was amplified from genomic DNA using the primer pair 3′UTR Mic2 fw/rv, and the PCR fragment was cloned into *p5RT70loxPKillerRedloxPYFP–HX* via SacI. The *mic2* ORF (TGME49_201780) was amplified from cDNA using the primers Mic2 ORF fw/rv, and was cloned into the parental vector *p5RT70loxPKillerRedloxPYFP–HX* using EcoRI and Pac1. Finally the *mic2* 5′UTR was amplified from genomic DNA using the primer pair 5′UTR Mic2 fw/rv, and cloned into the final vector using ApaI and EcoRI.

The *loxPAct1loxP–YFP–HX* construct was generated using the strategy described for *loxPMic2loxP–YFP–HX* with minor alterations. Firstly, the *act1* ORF (TGME49_209030) was amplified from cDNA using the primers Act1 ORF fw/rv and then the resulting PCR product was cloned into the parental vector *p5RT70loxPKillerRedloxPYFP–HX* using EcoRI and Pac1. To put *act1* under the control of the endogenous promoter a 2 kb fragment upstream of the start codon of *act1* was amplified from genomic DNA using the oligos 3′UTR Act1 fw/rv and cloned into the parental vector using EcoRI and PacI. Finally the *act1* 3′UTR was amplified from genomic DNA using the primer pair 3′UTR Act1 fw/rv, and cloned into the final vector using ApaI and EcoRI.

Generation of parasite lines

For the LacZ reporter strain, *pLox–P30/11LacZ–Lox–Tub5CAT* [17] was inserted randomly into RH *hxgprt*⁻ genome and positive clones were selected based on chloramphenicol resistance. Subsequently, *p5RT70FKBPCre59–DHFR* (30 μg DNA) and *p5RT70FRBCre60–HX* (60 μg DNA) were co–transfected and selected by pyrimethamine,

resulting in the strain RH *hxgprt*⁻ /*loxPlacZloxP/FKBPCre59/FRBCre60*, (referred to here as BloxP).

To generate a DiCre recipient strain expressing both subunits in the same genomic locus, *p5RT70DiCre–HX* was transfected into RH *hxgprt*⁻ (RH *hxgprt*⁻/*diCre*, referred to here as RH DiCre). Expression of Cre subunits was confirmed by Western blot analysis with antibodies against FKBP12 (Thermo Scientific: 1:500 dilution) and FRB (Enzo Life Sciences; 1:1000).

The *ku80::diCre* recipient strain was generated by replacing *hx* by *diCre* in the *ku80::hx* strain by homologous recombination (*ku80::hx*::*diCre*, referred to here as *ku80::diCre)*. The *5′UTR–DiCre–ku80 3′UTR* cassette was transfected into *ku80::hx* strain and subsequently *ku80::diCre* parasites were selected using 6–thioxanthine (i.e. absence of *hx* ORF). Integration of *diCre* into *ku80* locus was confirmed by analytical PCR on genomic DNA using ku80::hx fw (1)/ ku80 rv (1′) primer pair to check for the presence of *hx* in *ku80* locus. The conditional *myoA* KO strain (*RH DiCre/myoA::cat/loxPtymyoAloxP*, referred to here as loxPMyoA) was generated in three steps. Initially, a floxed transgenic copy of *myoA* was randomly integrated into RH DiCre recipient strain. To this end, the plasmid *p5RT70loxPTyMyoAloxP–DHFR* was transfected which confers pyrimethamine resistance. Secondly, the endogenous copy of *myoA* was replaced with the *cat* selection cassette by double homologous recombination using *pTgMyoA–KO–CAT* 3. The resulting loxPMyoA strain carries only one copy of *myoA* which was confirmed by PCR with the primers MyoA fw and rv that amplify DNA between two exons of myoA. Additionally, Western blotting using α–Ty and α–MyoA antibodies was performed. The floxed *myoA* can be excised by adding rapamycin (50 nM for 8 hours) resulting in the *myoA* null mutant (*RH DiCre/ myoA::cat/tymyoA*⁻, referred to here as *myoA* KO. Confirmation of the site–specific recombination leading to the excision of *myoA* was confirmed by PCR using the following primer sets: MyoA fw (1)/ MyoA rv (1′) and UpstreamLoxP fw (2)/DownstreamLoxP rv (2′). All assays were performed 96 hours post induction of Cre–mediated recombination. Reintroduction of the expression vector *p5RT70loxPTyMyoAloxP–DHFR* was achieved in absence of drug selection to complement the loss of *myoA*, resulting in the parasite line *RH DiCre/myoA::cat/ tymyoA*⁻/*loxPtymyoAloxP* (referred to here as loxPMyoA *comp*).

The conditional *mic2 KO* strain (*ku80::diCre/endogenous mic2::loxPmic2loxP*, referred to here as loxPMic2) was generated by transfecting 60 μg of the plasmid *loxPMic2loxPYFP–HX* into the *ku80::diCre* parasites to replace the endogenous copy of *mic2*, and parasites containing stable integration of this construct were selected using XAN and MPA as previously described [19]. The resulting loxPMic2 strain carries only one copy of *mic2*, which can be excised by adding rapamycin (50 nM in DMSO for 4 hours prior to washout) to generate the *mic2* null mutant (*ku80::diCre/mic2*⁻ referred to here as *mic2* KO). The clonal *mic2* KO line was isolated by performing serial dilutions on the clonal induced loxPMic2 strain after 4 hours induction and subsequent removal of rapamycin. Analytical PCR on genomic DNA using the primers intMic2ORF fw (1) and intMic2ORF rv (1′) established the presence / absence of the *mic2* ORF. PCR using primers Mic2LoxPF (2) and Mic2 vector 5′ rv (2′) confirmed the 5′ UTR integration in both the loxPMic2 and *mic2* KO parasites and Cre–mediated recombination in the *mic2* KO parasites. The 3′ UTR integration was checked using the primers HX fw (3) and Mic2 3UTR rv (3′). Additionally, Western blotting using α– MIC2 and α–aldolase antibodies was performed.

The conditional *act1 KO* strain (*ku80::diCre/endogenous act1::loxPact1loxP*, referred to here as loxPAct1) was generated by transfecting 50 μg of the plasmid *loxPAct1loxPYFP–HX* into the *ku80::diCre* parasites to replace the endogenous copy of *act1.* After transfection parasites were selected for stable integration using XAN and MPA as described

previously [19]. After the selection process the parasite pool was serially diluted to isolate single clones. The resulting LoxPAct1 strain carries only the Cre inducible copy of *act1*, allowing excision of *act1* upon rapamycin addition (50 nM in DMSO for 2 – 4 hours prior to washout) to generate the *act1* null mutant (*ku80::diCre/act1*$^{-}$ referred to here as *act1* KO). To confirm that the endogenous genomic DNA of actin was replaced by the introduced cDNA, analytical PCR was performed using the primers Act1 ORF fw (1) and Act1 ORF rv (1′). Confirmation of 5′ UTR integration and site–specific recombination leading to the excision of *act1* was confirmed by PCR using the oligos Act1 5′UTR fw (2) and YFP rv. The 3′ UTR integration into the correct locus was analysed using the primers HX fw2 (3) and Act1 3UTR rv (3′).

Parasite lines, transfections and selection

T. gondii tachyzoites (RH*hxgprt*$^{-}$) were cultured in human foreskin fibroblasts (HFF) cells and maintained in Dulbecco's modified Eagle's medium (DMEM) supplemented with 10 % fetal calf serum, 2 mM glutamine and 25 μg / mL gentamicin. To generate stable transformants, 1×10^7 of freshly lysed RH *hxgprt*$^{-}$ parasites were transfected with 60 μg linearized DNA by electroporation. Selection based on chloramphenicol (1 μM in EtOH; *CAT*) [20] pyrimethamine (1 μM in EtOH; *PYR*) [16], mycophenolic acid (12.5 mg / mL in MeOH; MPA) / xanthine (20 mg / mL in 1M KOH; XAN) [19] and 6–thioxanthine (25 mg / mL in 0.3M NaOH) were performed as described earlier.

PCR, Western blotting and immunofluorescence analysis

In order to extract genomic DNA from *T. gondii* to use as a PCR template, parasites were pelleted and subsequently washed in PBS. DNA extraction was performed using Qiagen DNeasy blood and tissue kit according to manufacturer's protocol.

Western blot samples were obtained by spinning down extracellular parasites and incubating them with RIPA buffer (50 mM Tris–HCl pH 8; 150 mM NaCl; 1 % Triton X–100; 0.5 % sodium deoxycholate; 0.1 % SDS; 1 mM EDTA) for 20 min on ice to lyse the parasites. Afterwards samples were centrifuged for 30 min at 14,000 rpm at 4 °C and laemmli buffer was added to the supernatant. Unless indicated otherwise 10^6 parasites were loaded onto a SDS acrylamide gel and immunoblot was performed as described previously [1].

For immunofluorescence analysis, infected HFF monolayers grown on coverslips were fixed in 4 % paraformaldehyde for 20 mins at RT, followed by blocking and permeablisation (2 % BSA & 0.2 % Triton X–100 in PBS). The staining was performed using different combinations of primary antibodies for 1 h and followed by secondary Alexa Fluor 488, Alexa Fluor 350 or Alexa Fluor 594 conjugated antibodies for another 45 min, respectively (1:1000–1:3000, Invitrogen–Molecular Probes).

Equipment and settings

For image acquisition z–stacks of 2 μm increments were collected using a UPLSAPO 100 x oil (1.40NA) objective on a Deltavision Core microscope (Image Solutions – Applied Precision, GE) attached to a CoolSNAP HQ^2 CCD camera. Deconvolution was performed using SoftWoRx Suite 2.0 (Applied Precision, GE) and further processed using ImageJ 1.34r software and Photoshop (Adobe Systems Inc., USA). Image acquisition was also conducted using a 100 x oil objective on a Zeiss Axioskope 2 MOT+ microscope attached to a Hamamatsu Orca–ER digital CCD camera using OpenLab 5.5.2 software (Improvision), and further processed using ImageJ and Adobe Photoshop.

LacZ analysis

To determine the efficiency of DiCre, BloxP parasites were treated with 50 nM rapamycin or 1 μM Shield–1 for 6 hours and grown under normal growth conditions for 48 h. Freshly lysed parasites were then added onto a monolayer of HFF and fixed 20 h later. The presence of LacZ was assessed by adding X–Gal (5–Bromo–4–Chloro–3–Indoyl–β–D–galactopyranoside) as substrate. Intracellular parasites were then fixed in 4 % paraformaldehyde for 20 min and subsequently washed three times in PBS. Afterwards the samples were incubated with the staining solution for 30 min at 37 °C. The staining solution contains 6 mM potassium ferricyanide, 6 mM potassium ferrocyanide, 2 mM $MgCl_2$, 0.2 % Igepal, 0.1 % Na deoxycholate, 1:40 dilution of X–Gal solution (40 mg / mL in N–N–dimethylformamide) in PBS. Afterwards the samples were rinsed 5 times in PBS. Experiment was performed in triplicate and 200 vacuoles were counted using a 100 x objective.

Invasion assay

To investigate the invasion rates of the loxPMyoA parasites (uninduced and induced), parasites were treated with 50 nM rapamycin in DMSO for 8 hours and grown in HFF cell monolayers for 96 hours. Afterwards, uninduced and induced parasites were scratched, filtered and 1×10^5 parasites were inoculated onto HFF monolayers per well. Parasites were allowed to invade for one hour at normal growth conditions (37 °C, 5 % CO_2), extracellular parasites were washed away with PBS and parasites were incubated for another 24 hours. Cells were fixed in 4 % paraformaldehyde for 20 min followed by immunostaining with α–IMC1 and α–Ty antibodies. The number of invaded parasites was counted in 20 fields using a 100 x objective, and calculated as a percentage value of uninduced loxPMyoA parasites normalised to 100 %.

Egress assay

4×10^5 parasites (loxPMyoA uninduced and induced 96 h earlier) were grown in HFF monolayers on coverslips for 36 h. Media was exchanged for pre–warmed, serum–free DMEM supplemented with 2 μM A23187 (in DMSO) in order to artificially induce egress [21]. After 10 min cells were fixed and stained with antibodies as indicated. 200 vacuoles were counted for each condition in three assays.

Plaque assay

1000 freshly lysed parasites were added onto a confluent monolayer of HFF cells and incubated for 5 days. The HFF monolayer was washed in PBS and fixed in ice cold methanol for 20 min. Afterwards, the HFFs were stained with Giemsa (1:10 in water) for 45 min and finally washed in PBS (3 x 5 min). Since methanol destroys the YFP signal, the *act1* KO plaque assays were image without fixation to differentiate between YFP positive and negative parasites. To quantify the relative plaque size of the indicated strains after 5 days on HFF monolayers, the average size of 15 plaques was determined and displayed relative to *ku80::diCre* or RH *hxgprt*$^-$ ± s.d, respectively. Plaque area was assessed using Image J 1.34r software.

FACS analysis

Freshly lysed parasites (mixed population expressing *p5RT70loxPKillerRedloxPYFP–HX*) were pelleted and washed once in PBS. Parasites were resuspended in 1 ml of 4 % paraformaldehyde and incubated in the dark for 20 min. The suspension was then centrifuged, followed by another PBS wash. Finally, FACS buffer (1 % FCS in PBS supplemented by 1 mM EDTA) was added to achieve a final concentration of 1×10^6 parasites per ml. 10,000 events were counted using FACSCalibur Becton Dickinson LSRII.

FSC and SSC were detected as small and large angle scatter of the 488 nm laser. KillerRed was excited by the 561 nm laser and detected by a 585 / 15 band pass filter. The YFP was excited by the 488 nm laser and detected by a 530 / 30 band pass filter and 505 long pass filters. For quantification, total number of fluorescent parasites was considered 100%.

Supplementary Material

Refer to Web version on PubMed Central for supplementary material.

Acknowledgments

We thank D. Soldati–Favre (University of Geneva, Switzerland), C.J. Beckers (The University of North Carolina, USA), A. Scherf (Pasteur Institute, France), J.F. Dubremetz (University of Montpellier, France), V. Carruthers (University of Michigan, USA), B. Striepen (University of Georgia, USA) and D.L. Sibley (Washington University, USA) for sharing reagents. We thank the FACS facility of the Institute of Infection, Immunity and Inflammation at Glasgow University for their support. This work was supported by the Wellcome Trust. M.M. is funded by a Wellcome Trust Senior Fellowship [087582/Z/08/Z)]. N.A. is supported by an EviMalaR (European FP7/2007-2013, grant number 242095) PhD fellowship and S.E. was funded via MALSIG. The Wellcome Trust Centre for Molecular Parasitology is supported by core funding from the Wellcome Trust [085349].

References

1. Herm-Gotz A, Agop-Nersesian C, Munter S, et al. Nat Methods. 2007; 4(12):1003. [PubMed: 17994029]
2. Meissner M, Breinich MS, Gilson PR, et al. Curr Opin Microbiol. 2007; 10(4):349. [PubMed: 17826309]
3. Meissner M, Schluter D, Soldati D. Science. 2002; 298(5594):837. [PubMed: 12399593]
4. Buguliskis JS, Brossier F, Shuman J, et al. PLoS Pathog. 2010; 6(4):e1000858. [PubMed: 20421941]
5. Starnes GL, Coincon M, Sygusch J, et al. Cell Host Microbe. 2009; 5(4):353. [PubMed: 19380114]
6. Daher W, Soldati-Favre D. Curr Opin Microbiol. 2009; 12(4):408. [PubMed: 19577950]
7. Plattner F, Yarovinsky F, Romero S, et al. Cell Host Microbe. 2008; 3(2):77. [PubMed: 18312842]
8. Huynh MH, Carruthers VB. PLoS Pathog. 2006; 2(8):e84. [PubMed: 16933991]
9. Jullien N, Sampieri F, Enjalbert A, et al. Nucleic Acids Res. 2003; 31(21):e131. [PubMed: 14576331]
10. Bulina ME, Lukyanov KA, Britanova OV, et al. Nat Protoc. 2006; 1(2):947. [PubMed: 17406328]
11. Skillman KM, Diraviyam K, Khan A, et al. PLoS Pathog. 2011; 7(10):e1002280. [PubMed: 21998582]
12. D. Soldati Boothroyd CJ. Mol Cell Biol. 1995; 15:87. [PubMed: 7799972]
13. Shaw MK, Compton HL, Roos DS, et al. J Cell Sci. 2000; 113(Pt 7):1241. [PubMed: 10704375]
14. Fichera ME, Roos DS. Nature. 1997; 390(6658):407. [PubMed: 9389481]
15. Hettmann C, Herm A, Geiter A, et al. Mol Biol Cell. 2000; 11(4):1385. [PubMed: 10749937]
16. Donald RG, Roos DS. Proc Natl Acad Sci U S A. 1993; 90(24):11703. [PubMed: 8265612]
17. Brecht S, Erdhart H, Soete M, et al. Gene. 1999; 234(2):239. [PubMed: 10395896]
18. Huynh MH, Carruthers VB. Eukaryot Cell. 2009; 8(4):530. [PubMed: 19218426]
19. Donald RG, Carter D, Ullman B, et al. J Biol Chem. 1996; 271(24):14010. [PubMed: 8662859]
20. Kim K, Soldati D, Boothroyd JC. Science. 1993; 262(5135):911. [PubMed: 8235614]
21. Black MW, Arrizabalaga G, Boothroyd JC. Mol Cell Biol. 2000; 20(24):9399. [PubMed: 11094090]

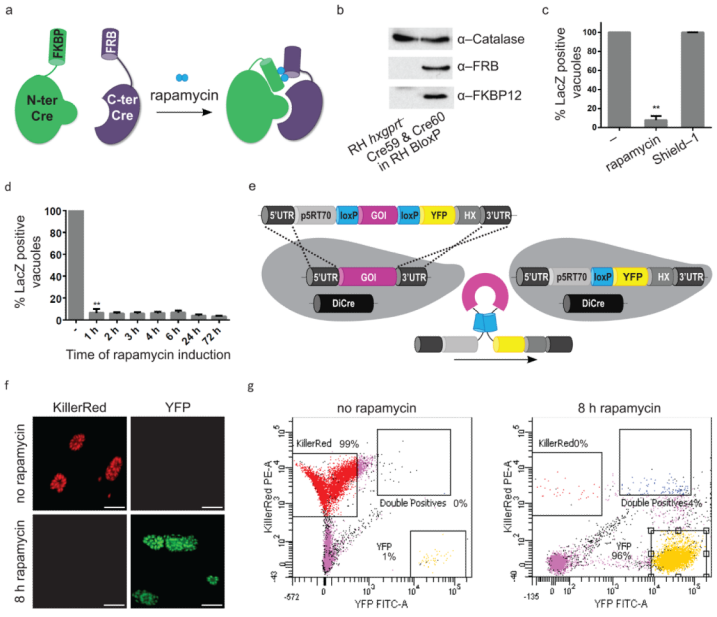

Figure 1. Establishing a conditional Cre–recombinase system in *T. gondii*

(**a**) Schematic of the DiCre system. Cre recombinase is split: Cre1–59 (green) is fused to FKBP12; Cre60–343 (purple) is fused to FRB. Rapamycin (blue) dimerizes subunits and reconstitute Cre activity. (**b**) Immunoblot analysis of DiCre expression using α–FKBP12 (19 kDa) and α–FRB antibodies (46 kDa) in *loxPlacZloxP* reporter parasite line (RH BloxP); α– Catalase (57 kDa) is the loading control. (**c**) Quantification of Cre–mediated recombination using 50 nM rapamycin or 1 μM Shield–1 for 6 h. Data from three experiments are shown, ±s.d., **: *P* value of 0.0008 in a two-tailed Student's t–test. (**d**) Quantification of Cre– mediated recombination over time. RH BloxP parasites expressing FKBP–Cre59 and FRB– Cre60 were treated with 50 nM rapamycin. LacZ expression is determined 72 hours post-induction. Data represents mean values of three independent experiments ±s.d, **: *P* value < 0.0001 in a two–tailed Student's t–test. **(e)** Schematic of the gene–swap strategy. The endogenous gene–of–interest (GOI, magenta) is replaced by the indicated cassette; the floxed GOI–cDNA is followed by YFP and the selectable marker (HX). Cre–mediated excision of GOI–cDNA places YFP under control of the promoter (p5RT70), producing green-fluorescent KO parasites. (**f,g**) Analysis of RH–DiCre transfected with *loxPKillerRedloxP– YFP*. Expression of KillerRed or YFP was analysed 5 days post–induction (50 nM rapamycin, 8 h in (**f**) immunofluorescence and (**g**) FACS analysis. Scale bar: 20 μm; 10,000 events were analysed by FACS.

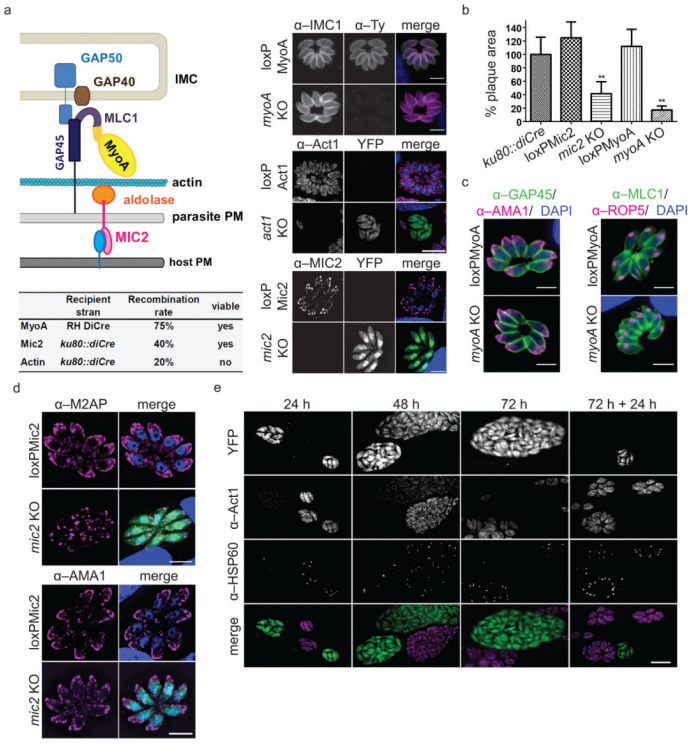

Figure 2. Utilizing the DiCre system to dissect the invasion machinery

(**a**) Current model of apicomplexan gliding and invasion machinery, and summary of KO parasites generated. Immunofluorescence analysis on the indicated KO strains demonstrates the complete absence of MyoA, MIC2 and Act1 respectively using the indicated antibodies. Scale bar: 5 μm. (**b**) Determination of plaque formation on a HFF monolayer by indicated parasite strains. The respective clonal KO strains (*mic2* KO and *myoA* KO), although viable *in vitro*, show a significant growth defect. Area of 15 plaques is assessed, **: *P* value < 0.0001 in a two–tailed Student's t–test. (**c**) Localisation of other invasion machinery components (MLC1 and GAP45) are not affected in *myoA* KO parasites, as shown in IFA using the indicated antibodies; scale bar 5 μm. (**d**) Localisation of M2AP but not AMA1 is disrupted in *mic2* KO parasites. IFA was performed using indicated antibodies, scale bar: 5 μm. (**e**) Actin is essential for apicoplast replication. loxPAct1 parasites were treated with rapamycin for 4 hours, inoculated on HFF cells, and imaged after the indicated time. Act1 protein levels are significantly reduced in green–fluorescent (*act1* KO) parasites after 24 hours and not detectable after 72 hours. The apicoplast, stained with α–HSP60, stops replicating, resulting in huge parasitophorous vacuoles containing few plastids. When parasites are artificially released from the host cell after 72 hours, YFP–expressing parasites can reinvade the host cell in absence of detectable Act1, but fail to replicate the apicoplast (72 h + 24 h). Scale bar: 5 μm.

Europe PMC Funders Author Manuscripts